

## Optical spectroscopy of molybdates with composition $\text{Ln}_2\text{Zr}_3(\text{MoO}_4)_9$ (Ln: Eu, Tb)

D. Sofich<sup>a,\*</sup>, Yu.L. Tushinova<sup>b</sup>, R. Shendrik<sup>a</sup>, B.G. Bazarov<sup>b</sup>, S.G. Dorzhieva<sup>b</sup>, O.D. Chimitova<sup>b</sup>, J.G. Bazarova<sup>b</sup>

<sup>a</sup> A.P. Vinogradov Institute of Geochemistry SB RAS, Russia

<sup>b</sup> Baikal Institute of Nature Management, SB RAS, Ulan-Ude, Russia



### ARTICLE INFO

#### Keywords:

Luminescence  
Molybdates  
Phosphors  
Spectroscopy  
Energy transfer

### ABSTRACT

This study examined the luminescent properties of systems of double molybdates doped with Eu and Tb — this includes emission, excitation and absorption spectra. The compounds exhibited bright luminescence in the visible region due to the  $[\text{Xe}]4f^n \rightarrow [\text{Xe}]4f^{n-1}$  transitions of rare-earth ions. The luminescence is excited both in the  $[\text{Xe}]4f^n \rightarrow [\text{Xe}]4f^{n-1}$  bands of the rare-earth ions and in the wide band in the ultraviolet region related to the transitions within the Mo-O complex. Because of the energy transfer, the luminescence of  $\text{Tb}^{3+}$  and  $\text{Eu}^{3+}$  in doubly doped molybdates has had common excitation energies.

### 1. Introduction

Sheelite-like compounds show promise as phosphors, scintillators and laser media which host lattice, are capable of storing a large amount of dopant due to highly distorted arrangement of anionic groups [1–5]. Molybdates doped with trivalent europium are excellent red phosphors and as such can be applied in three-color LEDs with effective ultraviolet pumping with near ultraviolet (NUV)-InGaN chips to the  $[\text{Xe}]4f^6 \rightarrow [\text{Xe}]4f^6 \text{Eu}^{3+}$  band  ${}^7\text{F}_0\text{--}{}^5\text{L}_6$  (395 nm) [6,7]. Studies have also shown that terbium molybdates are good luminophores; the luminescence  $[\text{Xe}]4f^8 \rightarrow [\text{Xe}]4f^8$  bands are distributed in a wide spectral region with their maximum in the green region. For practical application of these materials, it is important to know the color of the luminescence of a rare-earth ion (REI) for a particular matrix, or one would need to be able to change the color of the phosphor. Two types of molybdate powders with terbium and europium ions can be used to obtain a different color of luminescence, which is similar to how RGB (tri-color) LEDs work. Otherwise, we can synthesize a molybdate powder, doped twice with terbium and europium. In the luminescence spectrum of such a material, bands characteristic of both ions will be present, but in this case we do not know exactly how the ions will interact with each other. In this paper we discuss the results of spectroscopic studies of trivalent rare-earth ions in a matrix of double zirconium molybdate. The REI-REI and REI-host lattice interactions are described, and some parameters important for practical application are calculated.

### 2. Material and methods

The molybdate powders with composition  $(\text{Eu}_x\text{Tb}_{1-x})_2\text{Zr}_3(\text{MoO}_4)_9$  ( $x = 1, 0.9, 0.5, 0.1, 0$ ) were synthesized according to the ceramic technology by stepwise annealing a mixture of the stoichiometric amounts of  $\text{Eu}_2\text{O}_3$ ,  $\text{Tb}_4\text{O}_7$ ,  $\text{MoO}_3$  and  $\text{ZrO}_2$  for 150 h to a maximum temperature of 700 °C, according to the procedure described in Ref. [8]. The measured X-ray diffraction pattern for  $\text{Tb}_2\text{Zr}_3(\text{MoO}_4)_9$  is shown in Fig. 1.

The crystal structure of the host lattice is a three-dimensional lattice in which the polyhedra  $\text{LnO}_9$  (Ln = Eu, Tb) and  $\text{ZrO}_6$  octahedra are arranged in a rhombohedral order, connected through common oxygen vertices of two types to bridge the Mo tetrahedrons.

The luminescence spectra were recorded with a double monochromator SDL-1 (LOMO) with 600 lines/mm grating and a photoelectron multiplier FEU-106; excitation was carried out using a high-pressure 150 W xenon arc lamp DKSH-150 through a MDR-2 monochromator with a diffraction grating of 1200 lines/mm. The powder was applied to a transparent, undoped LiF crystal. The PLE spectra were corrected due to varying intensity of exciting light. Measurements of the decay times of the luminescence were carried out with excitation of a pulsed argon lamp with a pulse duration of 1.5  $\mu\text{s}$ . Photoluminescence decay curves were recorded on Rigol DS1102E oscilloscope connected to the FEU-106 photomultiplier.

The photoluminescence excitation (PLE) spectra were measured with grating monochromators MDR2 and 150 W xenon arc lamp for

\* Corresponding author.

E-mail address: [sofich-dmitriy@mail.ru](mailto:sofich-dmitriy@mail.ru) (D. Sofich).

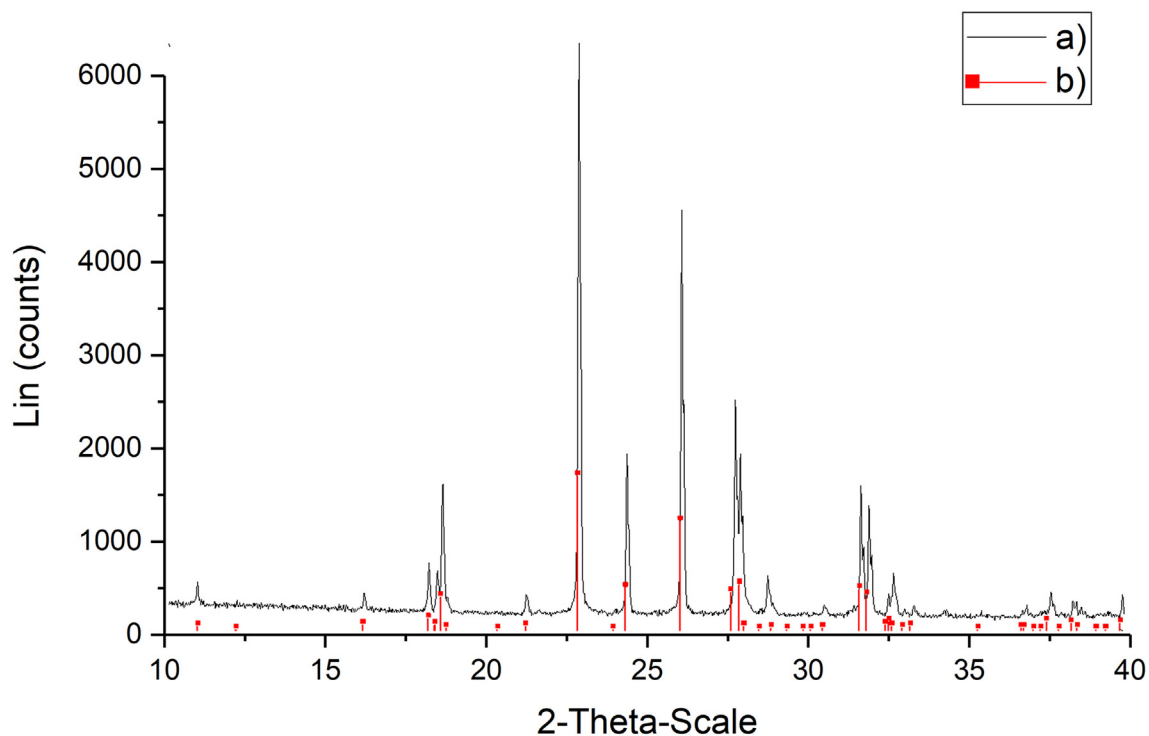


Fig. 1. Measured and calculated X-ray diffraction patterns of a)  $\text{Tb}_2\text{Zr}_3(\text{MoO}_4)_9$  b)  $\text{Eu}_2\text{Zr}_3(\text{MoO}_4)_9$ .

300–500 nm spectral region, a VM-2 (LOMO) vacuum monochromator, and a Hamamatsu deuterium lamp L7292 for measurements in the vacuum ultraviolet (VUV) spectral region. The optical absorption spectra were obtained by a Perkin-Elmer Lambda 950 UV/VIS/NIR spectrophotometer equipped with an integrating sphere at 300 K.

### 3. Results and discussion

The absorption spectra for the samples of  $\text{Tb}_2\text{Zr}_3(\text{MoO}_4)_9$  and  $\text{Eu}_2\text{Zr}_3(\text{MoO}_4)_9$  are given in Fig. 2.

Spectra show broad absorption bands at about 320 nm, identical for both samples, and the narrow weak bands are assigned to  $[\text{Xe}]4f^n \rightarrow [\text{Xe}]4f^{n-1}5d$  electronic transitions of the rare earth ions. The shortest wavelength line peaked at 395 nm corresponds to  $[\text{Xe}]4f^6 \rightarrow [\text{Xe}]4f^6$

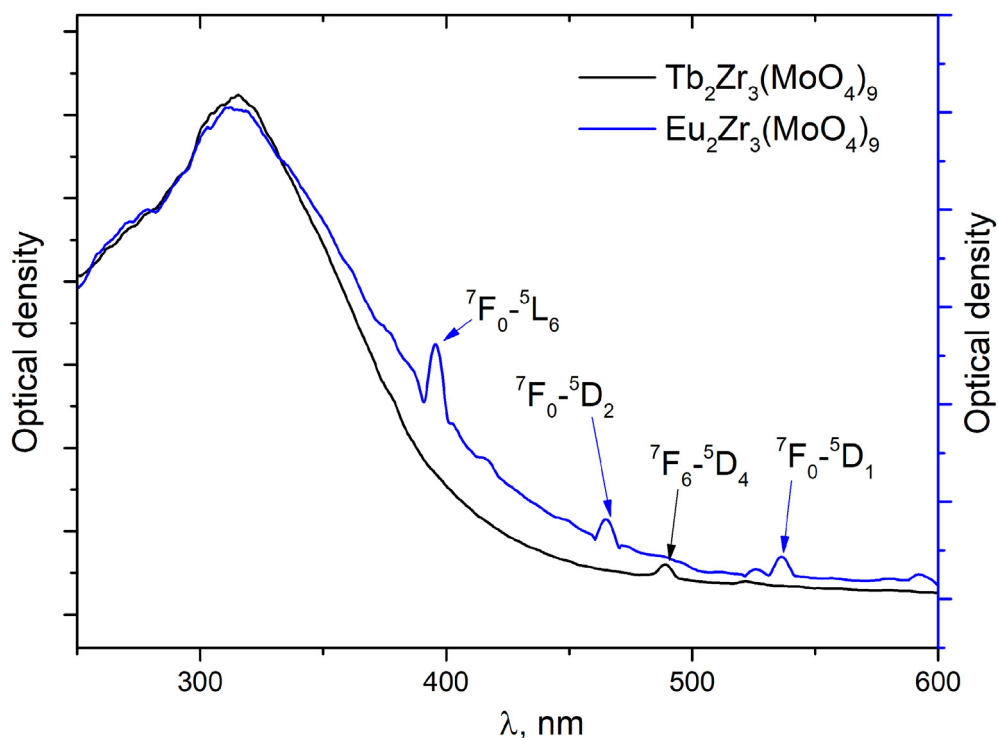


Fig. 2. The absorption spectra of  $\text{Tb}_2\text{Zr}_3(\text{MoO}_4)_9$  and  $\text{Eu}_2\text{Zr}_3(\text{MoO}_4)_9$ .

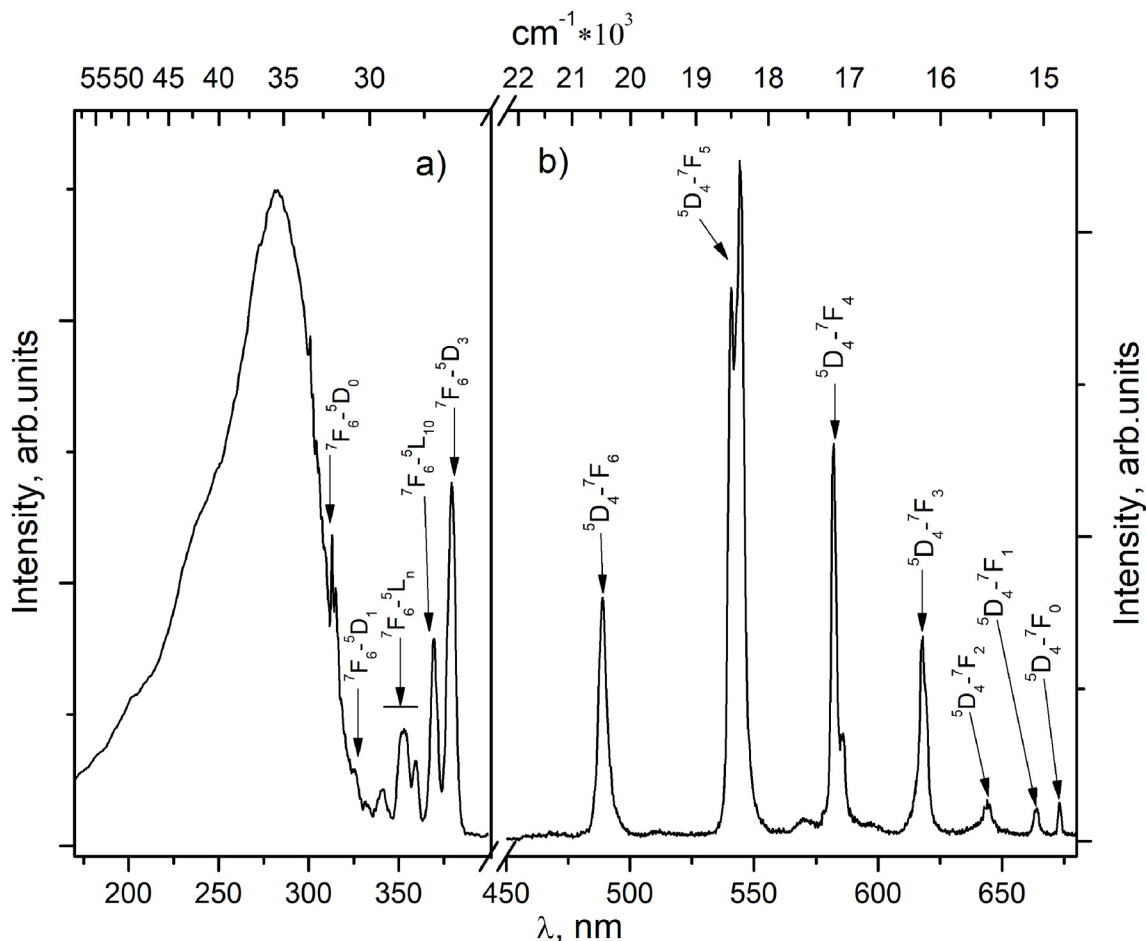


Fig. 3. The excitation (a) and luminescence (b) spectra of  $\text{Tb}_2\text{Zr}_3(\text{MoO}_4)_9$  at 545 nm emission and 379 nm excitation, respectively.

( ${}^7\text{F}_0$ - ${}^5\text{L}_6$ ) transition in  $\text{Eu}^{3+}$ . In  $\text{Tb}_2\text{Zr}_3(\text{MoO}_4)_9$  the shortest wavelength transition in absorption spectrum is attributed to term  ${}^7\text{F}_6$ - ${}^5\text{D}_1$  of  $\text{Tb}^{3+}$  ions.

Fig. 3 shows the excitation and luminescence spectra of  $\text{Tb}_2\text{Zr}_3(\text{MoO}_4)_9$ . Intense  $[\text{Xe}]4\text{f}^8 \rightarrow [\text{Xe}]4\text{f}^6$  emission bands are observed in the 480–680 nm region — these are typical for  $\text{Tb}^{3+}$  transitions from level  ${}^5\text{D}_4$  to the lower levels  ${}^7\text{F}_J$  ( $J = 0, 1, 2, 3, 4, 5, 6$ ). The  $[\text{Xe}]4\text{f}^8 \rightarrow [\text{Xe}]4\text{f}^6$  bands are narrow, with a half-width of 3–5 nm — this is due to the fact that the 4f-shell is screened by 5s and 5p electron shells in lanthanides. There are bands in the excitation spectrum that are associated with  $[\text{Xe}]4\text{f}^8 \rightarrow [\text{Xe}]4\text{f}^6$  transitions from the  ${}^7\text{F}_6$  ground state. When excited in the 4f<sup>8</sup>-bands, the highest luminescence intensity is achieved with the 380 nm excitation wavelength (transition  ${}^7\text{F}_6$ - ${}^5\text{D}_3$ ). The shortest wavelength narrow line corresponds to transition  ${}^7\text{F}_6$ - ${}^5\text{D}_0$ . In the region of 300 nm there is a wide intense excitation band. Seven narrow lines attributed to  $\text{Tb}^{3+}$  transitions -  ${}^5\text{D}_4$ - ${}^7\text{F}_6$  (490 nm),  ${}^5\text{D}_4$ - ${}^7\text{F}_5$  (543 nm),  ${}^5\text{D}_4$ - ${}^7\text{F}_4$  (582 nm),  ${}^5\text{D}_4$ - ${}^7\text{F}_3$  (618 nm),  ${}^5\text{D}_4$ - ${}^7\text{F}_2$  (644 nm),  ${}^5\text{D}_4$ - ${}^7\text{F}_1$  (663 nm) and  ${}^5\text{D}_4$ - ${}^7\text{F}_0$  (673 nm) – are all observed in emission spectrum. The most intensive line peaked at 543 nm causes green color of luminescence of the compound.

The luminescence spectrum of  $\text{Eu}_2\text{Zr}_3(\text{MoO}_4)_9$  (Fig. 4) consists of a set of thin bands around 591, 615, 651 and 691 nm corresponding to the  ${}^5\text{D}_0$ - ${}^7\text{F}_1$ ,  ${}^5\text{D}_0$ - ${}^7\text{F}_2$ ,  ${}^5\text{D}_0$ - ${}^7\text{F}_3$ ,  ${}^5\text{D}_0$ - ${}^7\text{F}_4$  transitions of  $\text{Eu}^{3+}$ . The  ${}^5\text{D}_0$ - ${}^7\text{F}_0$  emission at 583 nm is due to non-centrosymmetric site of europium [9]. Spectra show some weak emission from the  ${}^5\text{D}_1$  level of  $\text{Eu}^{3+}$ , around wavelengths 536, 556, 583 and 620 nm corresponding to transitions  ${}^5\text{D}_1$ - ${}^7\text{F}_1$ ,  ${}^5\text{D}_1$ - ${}^7\text{F}_2$ ,  ${}^5\text{D}_1$ - ${}^7\text{F}_3$ ,  ${}^5\text{D}_1$ - ${}^7\text{F}_4$  transitions, respectively. Those are associated with the multi-phonon relaxation process of  $\text{Eu}^{3+}$  [10].

The emission of  $\text{Eu}^{3+}$  is sensitive to local site symmetry. Authors [9]

described  ${}^5\text{D}_0$  to  ${}^7\text{F}_J$  ( $J = 0, 1, 2, 3, 4$ ) transitions for different inequivalent sites of  $\text{Eu}^{3+}$ . The  $\text{C}_4$  point group symmetry was determined for  $\text{Eu}^{3+}$  environment in  $\text{Eu}_2\text{Zr}_3(\text{MoO}_4)_9$ . Therefore, we assume the same group for  $\text{Tb}_2\text{Zr}_3(\text{MoO}_4)_9$ , due to similarity in host lattices. In the excitation spectrum the  $[\text{Xe}]4\text{f}^8 \rightarrow [\text{Xe}]4\text{f}^6$  transitions from the main 4f<sup>6</sup>-level ( ${}^7\text{F}_0$ ) are observed.

We studied  $(\text{Eu}_{0.9}\text{Tb}_{0.1})_2\text{Zr}_3(\text{MoO}_4)_9$ ,  $(\text{Eu}_{0.5}\text{Tb}_{0.5})_2\text{Zr}_3(\text{MoO}_4)_9$  and  $(\text{Eu}_{0.1}\text{Tb}_{0.9})_2\text{Zr}_3(\text{MoO}_4)_9$  compositions. The excitation and luminescence spectra were measured for different Tb/Eu ratios. Fig. 5 shows that the emission spectrum of  $(\text{Eu}_{0.1}\text{Tb}_{0.9})_2\text{Zr}_3(\text{MoO}_4)_9$  consists of a set of  $[\text{Xe}]4\text{f}^6 \rightarrow [\text{Xe}]4\text{f}^6$  lines related to the emission of  $\text{Eu}^{3+}$  and  $\text{Tb}^{3+}$  ions.

Fig. 6 presents the excitation and luminescence spectra of  $(\text{Eu}_{0.9}\text{Tb}_{0.1})_2\text{Zr}_3(\text{MoO}_4)_9$ ,  $(\text{Eu}_{0.5}\text{Tb}_{0.5})_2\text{Zr}_3(\text{MoO}_4)_9$ ,  $(\text{Eu}_{0.1}\text{Tb}_{0.9})_2\text{Zr}_3(\text{MoO}_4)_9$  compounds. The excitation spectra were recorded at a 616 nm emission band. This complex band consists of  ${}^5\text{D}_4$ - ${}^7\text{F}_3$  terbium and  ${}^5\text{D}_0$ - ${}^7\text{F}_2$  europium terms. The wide band in the excitation spectrum associated with the transitions inside the Mo-O complex does not change its shape and position at different concentrations of rare-earth ions. The ratio between the integrated intensity of  $[\text{Xe}]4\text{f}^n \rightarrow [\text{Xe}]4\text{f}^n$  bands and the Mo-O band for different concentrations of rare-earth ions in the excitation spectra remains unchanged. In the luminescence spectra, the intensity ratios of terbium and europium bands change as the ion concentrations change.

Fig. 7 shows the  $(\text{Eu}_{0.1}\text{Tb}_{0.9})_2\text{Zr}_3(\text{MoO}_4)_9$  spectra in the excitation and emission band characteristics of  $\text{Tb}^{3+}$  ions, while the vertical lines show the position of the main terms  $\text{Eu}^{3+}$ . The most intensive band in the excitation spectrum corresponds to the term  ${}^5\text{D}_4$ - ${}^7\text{F}_6$  (490 nm); bands characteristics of  $\text{Eu}^{3+}$  ions are present. The main  $\text{Eu}^{3+}$  transitions are allowed:  ${}^7\text{F}_0$ - ${}^5\text{L}_6$  (395 nm),  ${}^7\text{F}_0$ - ${}^5\text{D}_2$  (464 nm). The remaining

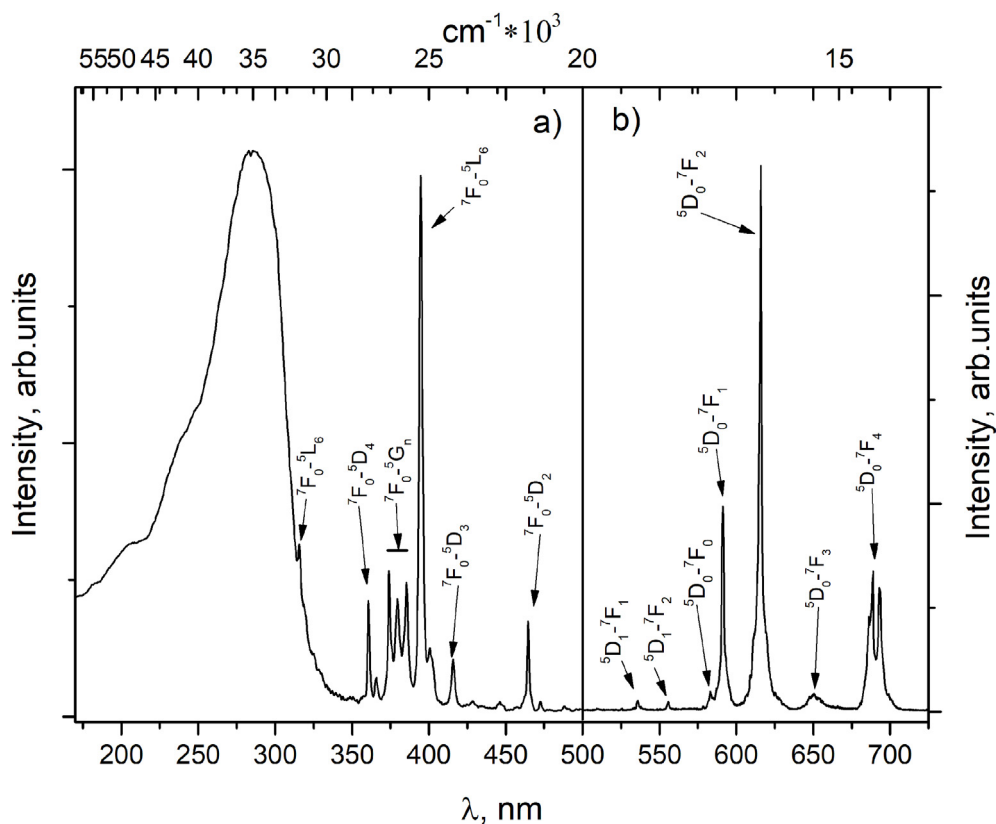


Fig. 4. The excitation (a) and luminescence (b) spectra of  $\text{Eu}_2\text{Zr}_3(\text{MoO}_4)_9$  at 615 nm emission and 395 nm excitation, respectively.

bands in the excitation spectrum are caused by the mixture of europium and terbium bands, with the main contributor being terbium. In the luminescence spectrum, the most intense bands are the europium  ${}^5\text{D}_0\text{-}{}^7\text{F}_1$ ,  ${}^5\text{D}_0\text{-}{}^7\text{F}_2$  and  ${}^5\text{D}_0\text{-}{}^7\text{F}_4$  bands. They are not resolved separately from the terbium bands, but from the position of the peaks we can

conclude that the main contribution to the luminescence ( $\text{Eu}_{0,1}\text{Tb}_{0,9}$ ) $\text{Zr}_3(\text{MoO}_4)_9$  gives  $[\text{Xe}]4f^6 \rightarrow [\text{Xe}] 4f^6$  the luminescence of  $\text{Eu}^{3+}$ . From the  $\text{Tb}^{3+}$  lines, only the  ${}^5\text{D}_4\text{-}{}^7\text{F}_5$  (543 nm) band is resolved apart from the europium lines.

Fig. 8a presents the decays of luminescence and decay times upon

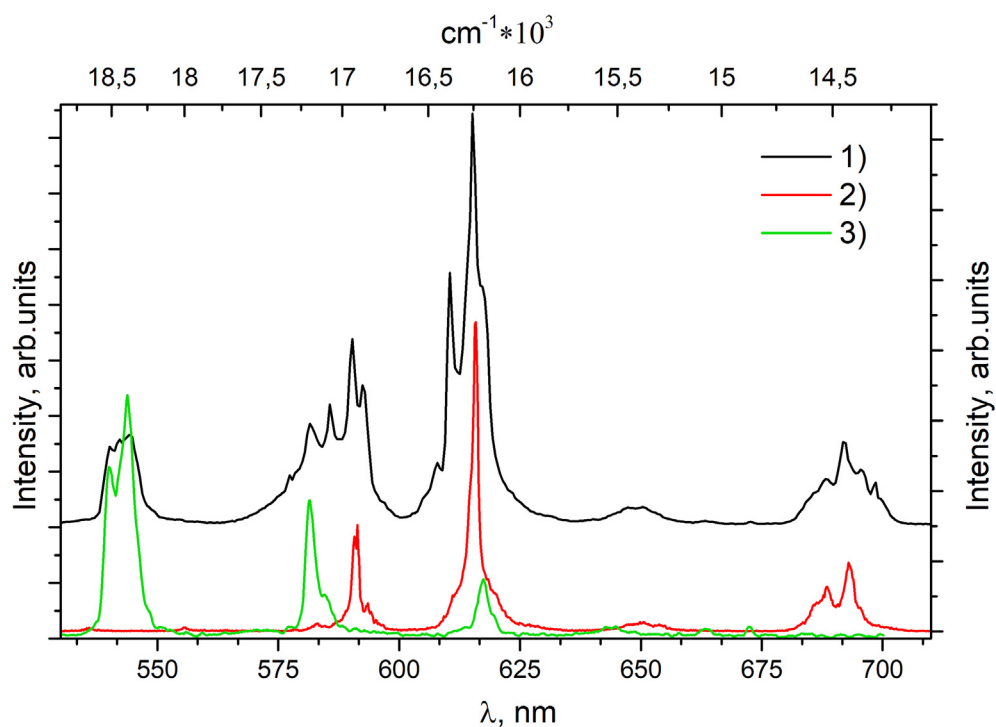


Fig. 5. Emission spectra for  $(\text{Eu}_{0,1}\text{Tb}_{0,9})_2\text{Zr}_3(\text{MoO}_4)_9$  (1),  $\text{Eu}_2\text{Zr}_3(\text{MoO}_4)_9$  (2),  $\text{Tb}_2\text{Zr}_3(\text{MoO}_4)_9$  (3).

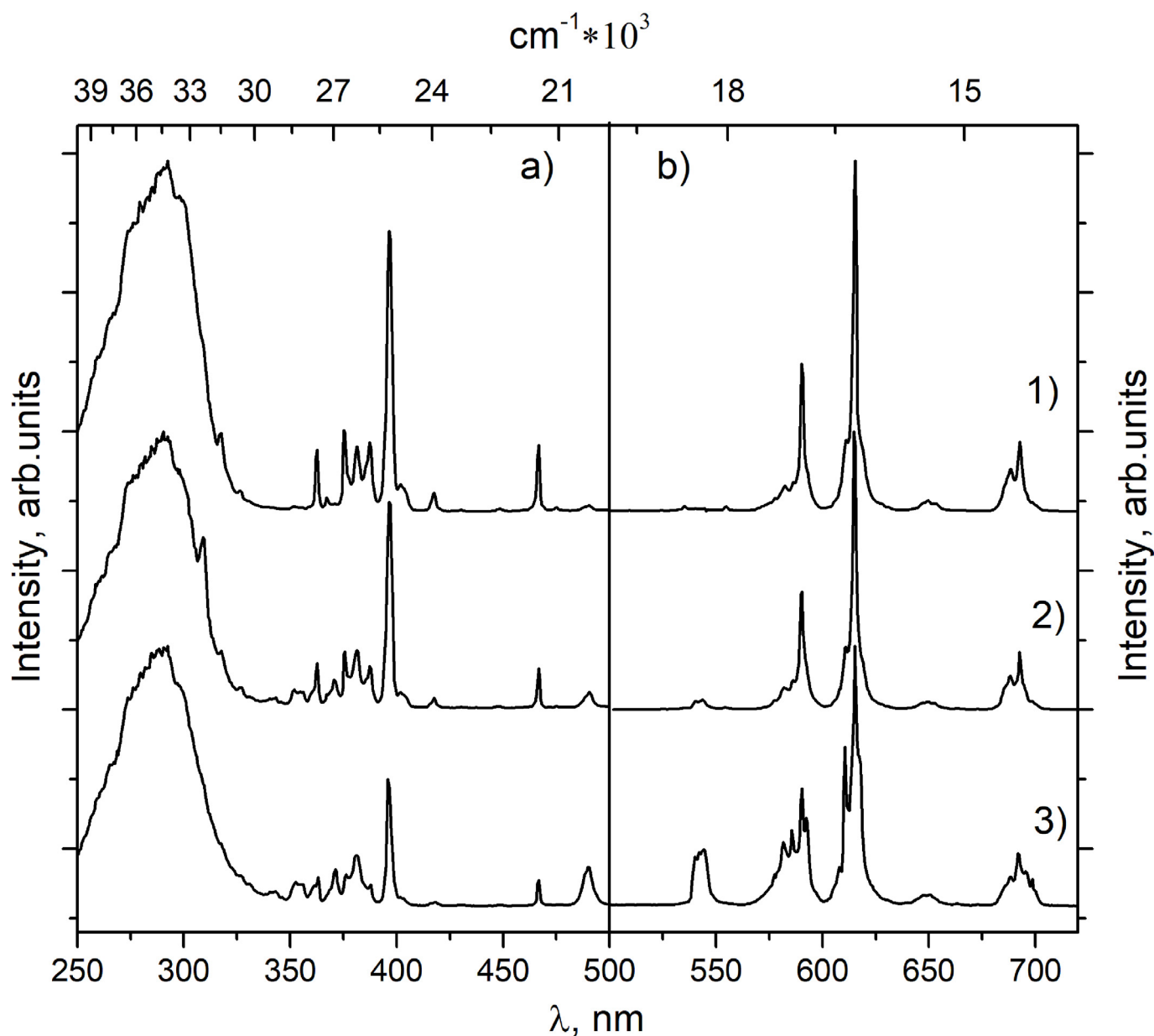


Fig. 6. Excitation and emission spectra of  $(\text{Eu}_{0.9}\text{Tb}_{0.1})_2\text{Zr}_3(\text{MoO}_4)_9$  (1),  $(\text{Eu}_{0.5}\text{Tb}_{0.5})_2\text{Zr}_3(\text{MoO}_4)_9$  (2),  $(\text{Eu}_{0.1}\text{Tb}_{0.9})_2\text{Zr}_3(\text{MoO}_4)_9$  (3) at 615 nm emission and 290 nm excitation, respectively.

excitation into the band 290 (Mo-O) nm and monitored at 615 nm ( $^5\text{D}_4\text{-}^7\text{F}_3$  and  $^5\text{D}_0\text{-}^7\text{F}_2$  optical transitions of  $\text{Tb}^{3+}$  and  $\text{Eu}^{3+}$  respectively). The collected decays are normalized to the signal intensity. With a decrease in the concentration of  $\text{Eu}^{3+}$ , decay time increases and decay curves slightly deviate from the monoexponential shape. The luminescence decay curves (Fig. 8b) measured at the maximum of their emission peak at 542 nm ( $^5\text{D}_4\text{-}^7\text{F}_5$  optical transition of  $\text{Tb}^{3+}$ ) are monoexponential in shape. The decay time increases with the increase in concentration of  $\text{Tb}^{3+}$ . Obviously, the largest contribution to the decay curve is provided by the luminescence of europium with a long lifetime. Measurements of the decays in the  $^5\text{D}_4\text{-}^7\text{F}_5$  terbium band (543 nm) gave the opposite result: with decreasing terbium concentration the decay time of the luminescence also decreases.

It can be concluded that there are several excitation transfer mechanisms in the compounds studied. We attribute a broad band in the excitation spectra to transitions within the Mo-O complexes with the subsequent energy transfer to the rare-earth ion. The independence of

the position and shape of the wide band for different rare-earth ions excludes the  $[\text{Xe}]4f^n \rightarrow [\text{Xe}]4f^{n-1}5d$  transitions from the list of possible ones. Also, other works [11–13] attribute such bands to transitions within the host. Another mechanism of energy transfer occurs between different types of rare-earth ions in these matrices. It was shown that europium ions are excited at  $^5\text{D}_4\text{-}^7\text{F}_6$  (490 nm) transition of  $\text{Tb}^{3+}$ . Conversely, in the excitation spectra of terbium, there are transitions from  $^5\text{D}_0$  to  $^7\text{F}_n$  terms characteristic for  $\text{Eu}^{3+}$  luminescence. It is worth noting that the transfer of energy between rare-earth ions proved to be more effective for the excitation of europium luminescence. A similar result is described in Ref. [14]. This is partly reflected in the color of the luminescence. Fig. 9 shows the chromaticity diagram, where a large prevalence in the luminescence of europium is seen even with a higher terbium concentration. It should be noted that the luminescence color of molybdates with  $\text{Eu}^{3+}$  has close parameters for red color to the common standards sRGB, HDTV, PAL/SECAM and NTSC.

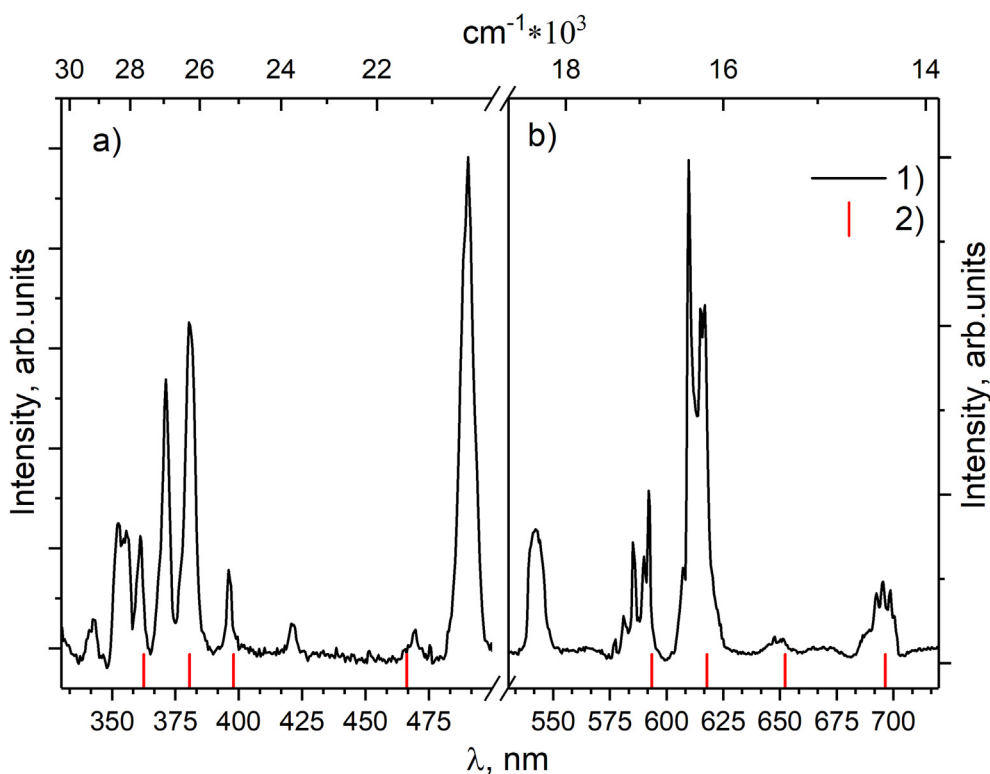


Fig. 7. Excitation and emission spectra  $(\text{Eu}_{0.1}\text{Tb}_{0.9})_2\text{Zr}_3(\text{MoO}_4)_9$  (1) at 543 nm emission and 490 nm excitation, respectively; and main europium bands (2).

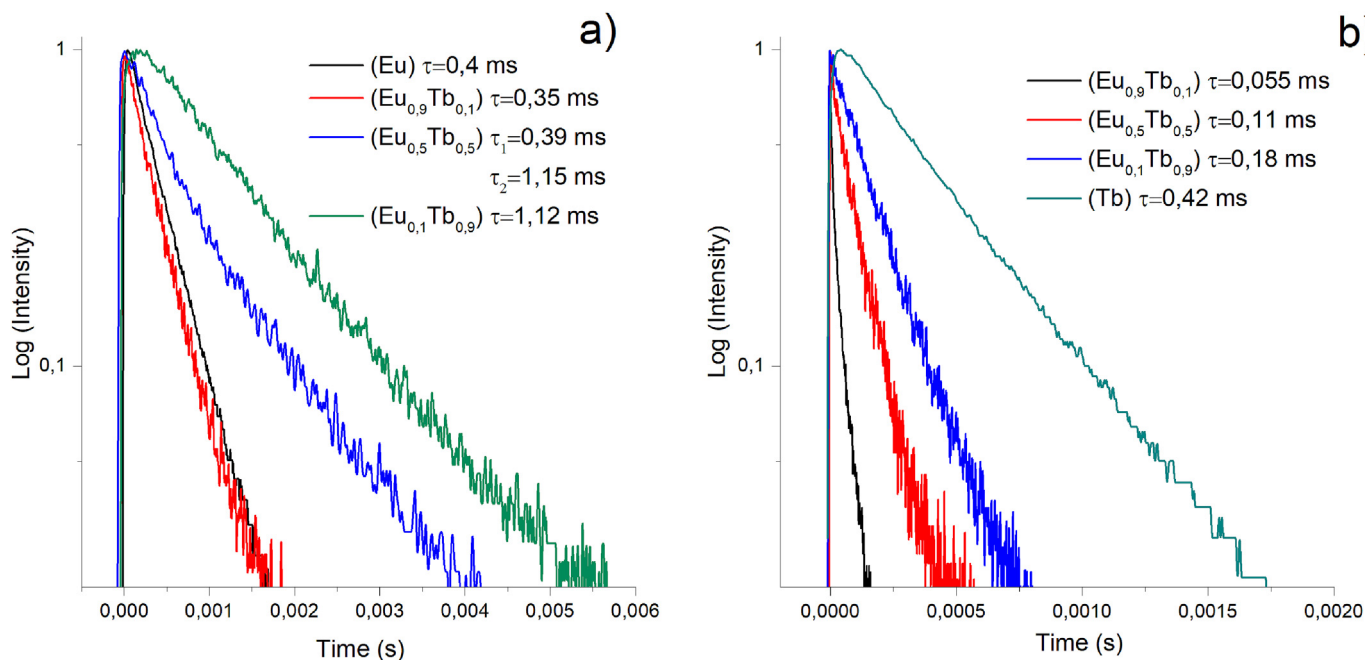


Fig. 8. Decays of the luminescence excited at 290 nm and monitored at 615 nm (a) and 542 nm (b).

#### 4. Conclusions

The studied double molybdates have a structure in which rare-earth ions occupy non-centrosymmetric sites, which affects their luminescent properties. The compounds have a broad absorption band in the 250–350 nm region and weak narrow absorption peaks of  $[\text{Xe}]4f^n \rightarrow [\text{Xe}]4f^{n+1}$  transitions, characteristic for trivalent Eu and Tb ions. There is an effective mechanism for transferring excitation from the crystal matrix to the rare-earth ion. The luminescence in the visible range is

completely due to the intraconfigurational  $[\text{Xe}]4f^n \rightarrow [\text{Xe}]4f^n$  transitions of rare-earth ions  $\text{Tb}^{3+}$  and  $\text{Eu}^{3+}$ .  $\text{Eu}_2\text{Zr}_3(\text{MoO}_4)_9$  has bright red luminescence, which is in good agreement with the NTSC standard. The luminescence of  $\text{Tb}_2\text{Zr}_3(\text{MoO}_4)_9$  is green with a slope of white color. Spectroscopic studies of doubly doped molybdates indicate that europium and terbium ions interact effectively. As has been shown, there is an effective mechanism for transfer of excitation of terbium ions to europium ions and vice versa.

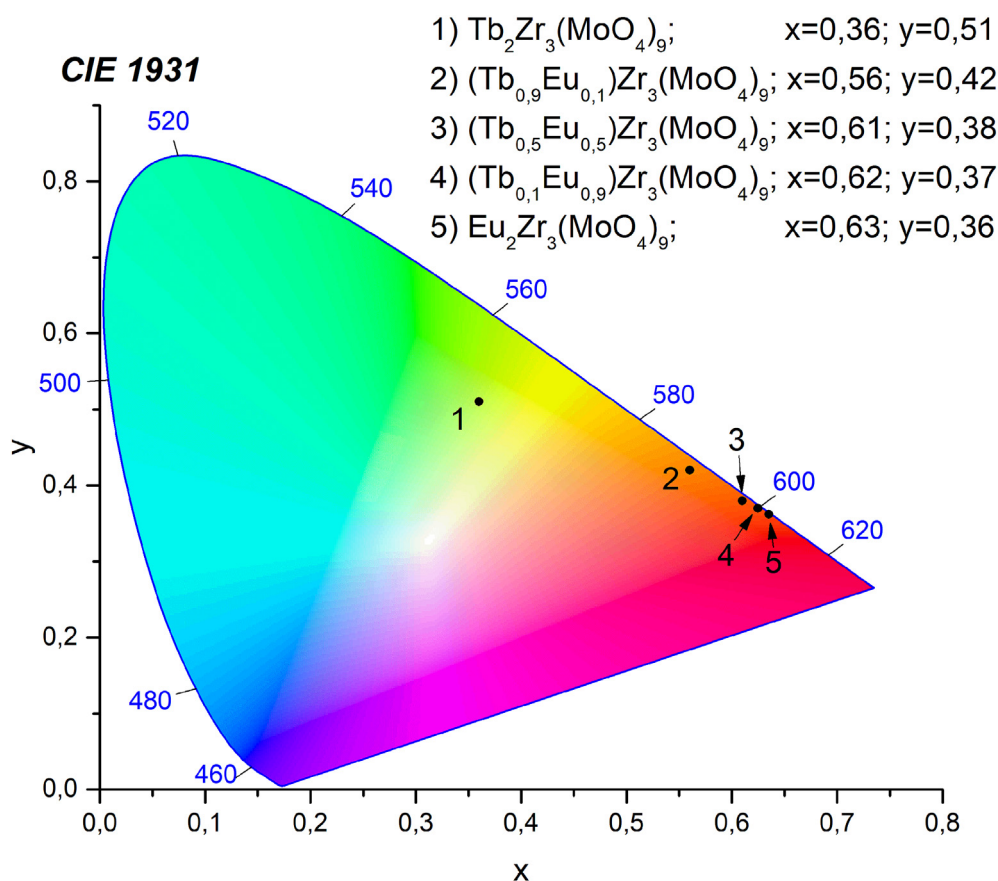


Fig. 9. CIE 1931 chromaticity diagram.

### Financial support

The present research was carried out according to the State assignment BINM SB RAS (project no.0339-2016-0007). This work was partly supported by RFBR grant 16-32-00198 mol\_a and a project no. 18-08-00799. Experimental setup was developed using governmental assignment in terms of Project IX.125.3 (0350-2016-0024, AA-17-117101170035-3). The study was supported by the Centers for Collective Use ("Isotope-geochemistry investigations" at A.P. Vinogradov Institute of Geochemistry SB RAS).

### References

- [1] Kasturi Singh, Sivakumar Vaidyanathan,  $\text{Li}_3\text{BaSrLa}_3(\text{WO}_4)_8$ :  $\text{Eu}^{3+}$  and its solid solutions: a new red emitting phosphor-structure, synthesis and appraisal of optical properties, *Chemistry* 2 (18) (2017) 5143–5156.
- [2] Chenning Zhang, et al., Prevention of thermal-and moisture-induced degradation of the photoluminescence properties of the  $\text{Sr}_2\text{Si}_5\text{N}_8$ : $\text{Eu}^{2+}$  red phosphor by thermal post-treatment in  $\text{N}_2$ - $\text{H}_2$ , *Phys. Chem. Chem. Phys.* 18 (18) (2016) 12494–12504.
- [3] N.M. Kozhevnikova, Synthesis and luminescence properties of a  $\text{Li}_3\text{BaCaY}_3(\text{MoO}_4)_8$ :  $\text{Er}^{3+}$  phosphor with a layered scheelite-like structure, *Inorg. Mater.* 53 (4) (2017) 419–423.
- [4] V. Mahalingam, et al., Potential visible light emitting rare-earth activated  $\text{Ca}_{0,5}\text{Y}_{1-x}(\text{MoO}_4)_2$ :  $x\text{RE}^{3+}$  (RE = Pr, Sm, Eu, Tb, Dy) phosphors for solid state lighting applications, *J. Mater. Sci. Mater. Electron.* 26 (2) (2015) 842–852.
- [5] D. Spassky, et al., Optical and luminescent properties of a series of molybdate single crystals of scheelite crystal structure, *Physica Status Solidi (C)* 2 (1) (2005) 65–68.
- [6] Kai-Shing Yang, et al., An experimental and analytical investigation of the photo-thermal-electro characteristics of a high power InGaN LED module, *Appl. Therm. Eng.* 98 (2016) 756–765.
- [7] Shuji Nakamura, et al., InGaN/GaN/AlGaN-based laser diodes with modulation-doped strained-layer superlattices grown on an epitaxially laterally overgrown GaN substrate, *Appl. Phys. Lett.* 72.2 (1998) 211–213.
- [8] S.G. Dorzhieva, Y.L. Tushinova, B.G. Bazarov, Z.G. Bazarova, A.I. Nepomniashchikh, R.Y. Shendrik, Luminescence of Ln-Zr molybdates, *Bull. Russ. Acad. Sci. Phys.* (2015) 276–279 T. 79. № 2.
- [9] Koen Binnemans, Interpretation of europium (III) spectra, *Coord. Chem. Rev.* 295 (2015) 1–45.
- [10] Yue Tian, et al., Self-assembled 3D flower-shaped  $\text{NaY}(\text{WO}_4)_2$ :  $\text{Eu}^{3+}$  micro-architectures: microwave-assisted hydrothermal synthesis, growth mechanism and luminescent properties, *CrystEngComm* 14 (5) (2012) 1760–1769.
- [11] M. Guzik, et al., Eu 3+ luminescence from different sites in a scheelite-type cadmium molybdate red phosphor with vacancies, *J. Mater. Chem. C* 3 (33) (2015) 8582–8594.
- [12] Pieter Dorenbos, Charge transfer bands in optical materials and related defect level location, *Opt. Mater.* 69 (2017) 8–22.
- [13] Matas Janulevicius, et al., Luminescence and luminescence quenching of highly efficient  $\text{Y}_2\text{Mo}_4\text{O}_{15}$ :  $\text{Eu}^{3+}$  phosphors and ceramics, *Sci. Rep.* 6 (2016) 26098.
- [14] Irene Carrasco, Fabio Piccinelli, Marco Bettinelli, Luminescence of Tb-based materials doped with  $\text{Eu}^{3+}$ : case studies for energy transfer processes, *J. Lumin.* 189 (2017) 71–77.